



*I. A. Mohammed-Dabo, S. I. Dederi, H. Nuhu

Department of Chemical Engineering, Ahmadu Bello University, Zaria, Nigeria.

Corresponding author: inuwa.dederi-salisu@dangoteprojects.com

Received: September 14, 2023 Accepted: November 28, 2023

Abstract: Emissions from combustion processes, particularly oxides of nitrogen (NO_x), carbon monoxide, and other pollutants, have substantial implications for both public health and environmental well-being. This research addresses the imperative of predictive emission monitoring through the development of a Parametric Emissions Monitoring System (PEMS) for gas-fired boilers. Focused on the equilibrium model for NO_x emissions during combustion, this study integrates thermodynamic, materials, and energy balance equations using advanced engineering software. The model's accuracy was validated through meticulous comparisons with field data from a UREA power plant in Nigeria, showcasing its reliability for predicting NO_x concentrations. Beyond its role in design and operations, the developed model contributes significantly to assessing and managing pollutant quantities. The study underscores NO_x as a primary concern and explores the impact of factors such as flame temperature and excess air quantity on NO_x formation. Practical implications of the research encompass the application of lean premix technology to control flame temperature and optimize excess air for NO_x reduction. This work enhances our understanding of gas-fired boiler emissions and provides a valuable tool for addressing environmental and regulatory challenges in industrial settings.

Keywords: Pentaclethra Macrophylla Feedstock, Transesterification, Biodiesel, Viscosity

Introduction

Industrial activities globally release substantial quantities of pollutants annually, contributing to severe health issues such as malignancies, neurological disorders, respiratory ailments, and reproductive problems (Manisalidis *et al.*, 2020). The emission levels of anthropogenic sources and air pollutants vary worldwide, influenced by a nation's technological development, standard of living, cultural beliefs, and implemented control strategies. Notably, power plants emerge as significant contributors to air pollution on a global scale (Okedere *et al.*, 2021). In 2014, Nigeria, a major contributor to greenhouse gas emissions, produced approximately 492.44 million metric tons of greenhouse gases (GHGs), accounting for 1.01% of global GHG emissions (USAID, 2012). The nation is a notable source of various air pollutants, including carbon monoxide (CO), nitrogen oxides (NO_x), particulate matter (PM₁₀), sulfur dioxide (SO₂), and volatile organic compounds (VOCs), emanating from diverse sources within petroleum refineries (Okedere *et al.*, 2021; USAID, 2012).

The surge in industrial activities, marked by increased numbers, sizes, and capacities, necessitates additional power supply infrastructure, such as turbine and generator systems, and steam boilers. While steam boilers operate on various fuels like diesel, petrol, wastes, and wood ashes (Coykendall *et al.*, 2012), the combustion of different sources yields varying concentrations and types of air pollutants. Sulfur dioxide (SO₂), nitrogen oxides (NO_x), and particulate matter stand out as primary hazardous air pollutants (HAPs), demanding heightened attention due to their adverse health impacts (Kitto & Beach, 2017; Manisalidis *et al.*, 2020). The deleterious effects of air pollution on climate change and public health underscore its status as a critical contemporary challenge (Manisalidis *et al.*, 2020). Numerous contaminants, including Particulate Matter (PM) with its small diameter, contribute significantly to human diseases, affecting the respiratory, cardiovascular, and reproductive systems, and even posing cancer risks (Lu, 2021). High concentrations of ground-level ozone further exacerbate

respiratory and cardiovascular issues (Jeevan *et al.*, 2022; Manisalidis *et al.*, 2020). The escalating concern over atmospheric pollution has led to the enactment of stringent global environmental regulations. To meet these regulations, especially for SO₂ and NO_x, diverse air quality control technologies, such as selective catalytic reduction (SCR), selective non-catalytic reduction (SNCR), adsorption, flue gas desulfurization (FGD), and various scrubbing systems, have been developed (Ness *et al.*, 2021; Xu *et al.*, 2020). However, effective emission monitoring remains a challenge for government agencies, with instances of industries deceiving regulators. Notable cases, like the Volkswagen emission scandal, underscore the need for robust monitoring and regulatory enforcement to ensure compliance and mitigate environmental and public health impacts (JusticeNews, 2016; USEPA, 2022).

Moreover, the exposure to Particulate Matter (PM_{2.5}) and NO_x has been linked to myopia, as revealed in a study by Yang *et al.* (2020). Methods for estimating emissions, such as Continuous Emission Monitoring System (CEMS) and Predictive/Parametric Emission Monitoring (PEM), play a crucial role in compliance assessment. The choice between these methods depends on factors like time specificity, data quality, and the type of emissions under consideration (Davison *et al.*, 2020; Kusek & Rist, 2004). While CEMS is the preferred method for annual emission inventories, PEM provides accurate estimates but is contingent on the availability of continuous measurement data.

Materials and Method

Block flow diagram

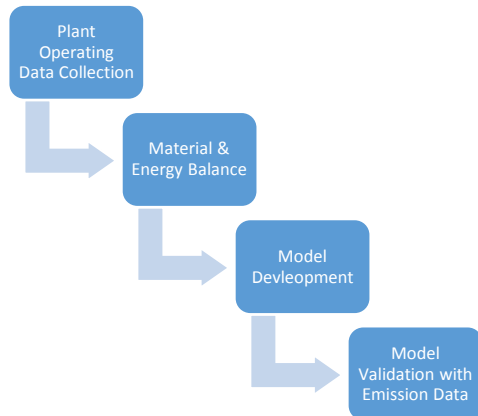


Figure 1: Block flow diagram of methodology

Plant Operating Data Collection

Fuel

Natural gas, obtained from the Nigerian Gas Company via the Excravos-Lagos Pipeline System, served as the primary fuel. The molar composition of the natural gas is detailed in Table 1.

Table 1: NGC (Excravos-Lagos Pipeline System) natural gas molar composition

Component	Molar Composition (%)
Methane (CH ₄)	86.66
Ethane (C ₂ H ₆)	6.08
Propane (C ₃ H ₈)	2.13
Nitrogen (N ₂)	0.73
Carbon Dioxide (CO ₂)	3.12
i-butane	0.39
n-butane	0.4
i-pentane	0.08
n-pentane	0.18
n-hexane	0.23

Plant Operating Conditions of the Utility Boilers in Case Study

The utility boilers in the urea plant, three 40MW steam water tube fired boilers, operated under conditions outlined in Table 2.

Table 2: Utility Boiler Plant Operating Parameters

Parameter	Value
Boiler Type	Water Tube
Capacity	40MW (each)
Fuel	Natural Gas
Combustion air temoerature	307K
Combustion air flowrate	63.96 kg/s
Fuel gas mass flow rate	6.82 kg/s

Parameter	Value
Fuel gas inlet temperature	328K
Air/fuel ratio at full load	15/1
Specific heat capacity of air	1.005 kJ/kgK
Specific heat capacity of gas	1.15 kJ/kgK

Material Balance

Assumptions to be considered

In formulating the material balance for the system, certain assumptions were made:

1. There is sufficient residence time to achieve perfect mixing of air and fuel.
2. Combustible components in natural gas undergo complete combustion.
3. The composition of 1 kmol of air is 0.79 kmol of nitrogen and 0.21 kmol of oxygen.
4. The oxygen available for thermal fixation with nitrogen to form NO_x is the excess oxygen in the combustion chamber after the stoichiometric reaction.
5. NO_x production occurs in the combustor after achieving adequate temperature for nitrogen and oxygen fixation.

The general material balance equation for a system, considering chemical reactions, is expressed as:

$$A=I-O+G-C \quad (1)$$

Where:

- *A* is the accumulation within the system,
- *I* is the input into the system,
- *O* is the output through the system boundary,
- *G* is the generation within the system,
- *C* is the consumption within the system (Himmelblau, 2004).

As the system operates at steady state (*A*=0), the material balance simplifies to:

$$O=I+G-C \quad (2)$$

Considering the law of conservation of mass, which dictates that generation and consumption are zero, equation (2) further simplifies to:

$$O=I \quad (3)$$

Energy Balance

The law of conservation of energy states that energy can neither be created nor destroyed but transformed. For a steady flow system, the general energy equation, neglecting changes in kinetic and potential energy, is given by:

$$Q+W=HP_{(2)}-HR_{(1)} \quad (4)$$

Where:

- *Q* is the heat supplied to the system from the surroundings,
- *W* is the work done by the surroundings on the system,
- *HP₍₂₎* is the enthalpy of products at state 2,
- *HR₍₁₎* is the enthalpy of reactants at state 1.

With a change in reference temperature and assuming an adiabatic process with no flow work done, the steady flow energy equation can be rewritten as:

$$HP(T2)-HP(25)+\Delta H_{0rxn}(25)+HR(25)-HR(T1)=0 \quad (5)$$

$$(T2) - HP(25) + \Delta H_{0rxn}(25) + HR(25) - HR(T1) = 0 \quad (6)$$

Where $\Delta H_{0rxn}(25)$ is the enthalpy of reaction at 25°C. The energy equation is further detailed with the specific heat capacity (C_p) and temperature change (ΔT):

$$H = m \cdot C_p \cdot \Delta T \quad (8)$$

Where:

- m is the mass flow,
- C_p is the specific heat capacity at constant pressure,
- ΔT is the change in temperature.

The steady flow energy equation (6), combined with the material balance equation (3), was employed to calculate the adiabatic flame temperature on Microsoft Excel 2019, serving as the foundation for the NOx dissociation model development.

The summarized material and energy balance data for Boiler A and Boiler B are presented in Table 3.

Table 3: Material and Energy balance data

Components	BOILER A	BOILER B
Nitrogen (air + fuel) nN2	10.3177	6.8101
Oxygen O2 (Excess) nO2	1.9900	0.0484
Combustion Products nt	13.4355	6.9583
Enthalpy of air Ha(40.35)	254670.3kJ	124654.39kJ
Enthalpy of fuel Hf(54.85)	4627.7kJ	26592.0kJ
Enthalpy of reactants at inlet conditions Hr(in) = Ha + Hf	259298.319kJ	147513.391kJ
Enthalpy of reaction $\Delta H_{rx}(25)$	-303202.1kJ	-742884kJ
Enthalpy of products Hp(25)	118718.404kJ	22867.815kJ
Enthalpy of reactants Hr(25)	117557.127kJ	

Combustion Simulation with Aspen Hysys

The combustion process was meticulously simulated using Aspen Hysys Software V8.4, employing a perfectly mixed reactor model. The Peng Robinson Equation of State, known for its accurate property correlations, was selected. All combustion reactions were precisely specified in the reaction package using fundamental hydrocarbon combustion equations.

The pressures and temperatures of each component utilized are detailed in Table 2. The simulation results are vividly presented in Figure 2.

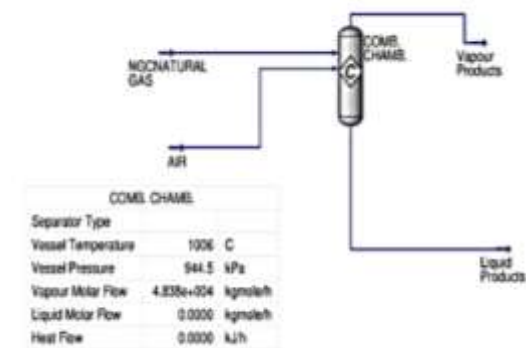


Figure 2: Combustion simulation of the gas-fired boiler using Aspen Hysys

Figure 2 showcases the outcome of the combustion simulation performed with Aspen Hysys V8.4. The combustion chamber registers a temperature of 1006 °C and a pressure of 944.5 kPa. The molar flow of the products is measured at 48380 kmol/h, with no liquid molar flow observed, given that all components exist in the vapor state at the elevated system temperature. Additionally, assuming an adiabatic process, there is no heat flow into or out of the system.

NOx Correlation

An equivalent thermal equilibrium expression for NO based on the reaction $1/2N_2 + 1/2O_2 \rightleftharpoons NO$ is given by:

$$K_{eq}^{\theta} = \frac{(p_{NO})}{(p_{O_2})^{\frac{1}{2}} * (p_{N_2})^{\frac{1}{2}}} \quad (9)$$

Here: k_{eq} is the thermal equilibrium constant or dissociation constant.

p_{NO} is the partial pressure of NO
 p_{N_2} is the partial pressure of N_2
 p_{O_2} is the partial pressure of O_2

Nitric oxide (NO) being the primary oxide of nitrogen formed by high temperature fixation of nitrogen and oxygen, may undergo further conversion to other oxides of nitrogen after its formation. This work accounts for oxides of nitrogen formation by considering the quantity of NO producible at thermodynamic equilibrium. Equation (9) is further expressed as Equation (10):

$$p_{NO} = K_{eq}^{\theta} * (p_{O_2})^{\frac{1}{2}} * (p_{N_2})^{\frac{1}{2}} \quad (10)$$

From Dalton's law of partial pressure,

$$p_i = \frac{n_i}{n_t} * P_t$$

Where:

p_i is the partial pressure of a component, P_t is the system total pressure; n_i is the number of moles of a component, and n_t is the total number of moles of all components in the system.

Relating Equations (10) and (11), an equivalent expression becomes:

$$\frac{n_{NO}}{n_t} * P_t = K_{eq}^{\theta} * \left(\frac{n_{O_2}}{n_t}\right)^{\frac{1}{2}} * P_t^{\frac{1}{2}} * \left(\frac{n_{N_2}}{n_t}\right)^{\frac{1}{2}} * P_t^{\frac{1}{2}}$$

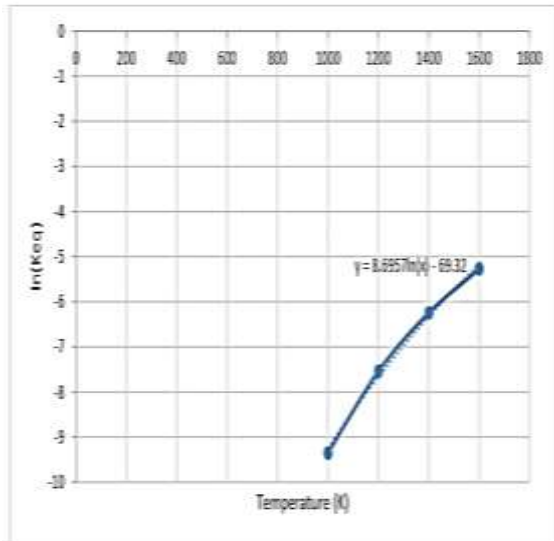
On simplification of Equation (12) a resulting equation is given by Equation (13):

$$\frac{n_{NO}}{n_t} * P_t = K_{eq}^{\theta} * (n_{O_2})^{\frac{1}{2}} * (n_{N_2})^{\frac{1}{2}} * \frac{P_t}{n_t} \quad (13)$$

By further simplifying Equation (13); Equation (14) is derived and is given by:

$$\frac{n_{NO}}{n_t} = K_{eq}^\theta * \frac{(n_{O2} * n_{N2})^{\frac{1}{2}}}{n_t} \quad (14)$$

Now, since mole fraction of a component 'yi' is given by the expression:



$$y_i = \frac{n_i}{n_t}$$

Equation (14) can be rewritten as:

$$y_{NO} = K_{eq}^\theta * \frac{(n_{O2} * n_{N2})^{\frac{1}{2}}}{n_t} \quad (16)$$

To establish an expression for the equilibrium constant K_{eq} , experimental data for the operating temperature range, extracted from thermodynamic and transport properties of fluids compiled by Rogers and Mayhew, is presented in Table 4. Analysis of the data in Table 4, using Microsoft

Table 5: Comparison of NOx emission from predicted model and plant data pre commissioning (Boiler A)

Monthly NOx ppm	Average NOx (ppm)	Conc. Developed model (ppm)	Deviation	Percentage Deviation
August 2020	52.6	49.148	3.452	6.563
Sept. 2020	55.2	53.046	3.154	3.902
Oct. 2020	55.8	53.621	2.179	3.905

Table 6: Comparison of NOx emission from predicted model and plant data post commissioning (Boiler A)

Monthly NOx ppm	Average NOx (ppm)	Conc. Developed model (ppm)	Deviation	Percentage Deviation
April 2021	132	127.737	4.263	3.230
May 2021	135	131.864	3.154	2.336
June 2021	131	127.912	3.088	2.357

Excel, yields a robust correlation for $\ln K_{eq}$, as depicted in Figure 3.

Table 4: Natural logarithm of equilibrium constant for NO

Temperature (K)	$\ln K_{eq}^\theta$
1000	-9.353
1200	-7.541
1400	-6.245
1600	-5.273

Figure 3: NOx correlation of $\ln K_{eq}^\theta$ with temperature

From the correlation equation in Figure 3,

$$I(K_{eq}^\theta) = 8.6957 \ln(T) - 69.32 \quad (17)$$

Consequently,
$$K_{eq}^\theta = \exp^{(8.6957 \ln(T) - 69.32)} \quad (18)$$

Combining Equations (16) and (18), the expression developed for NOx in this research work is given by:

$$y_{NOx} = \exp^{(8.6957 \ln(T) - 69.32)} * \frac{(n_{O2} * n_{N2})^{\frac{1}{2}}}{n_t} \quad (19)$$

Where:

y_{NOx} = mole fraction of NOx in the exhaust

T = combustor temperature (K)

n_{O2} = amount of oxygen in products stream (kmol/s)

n_{N2} = amount of nitrogen in products stream (kmol/s)

n_t = total amount of products. (kmol/s)

Results and Discussion

Comparison of Models with Plant Data

The correlations outlined in Chapter three were meticulously solved using Excel and MATLAB software, and the results and deductions are systematically presented in Tables 5 through 7.

Table 7: Comparison of NOx emission from predicted model and plant data post commissioning (Boiler B)

Monthly average NOx ppm	NOx (ppm)	Conc. Developed model (ppm)	Deviation	Percentage Deviation
May 2021	175.915	168.172	7.743	4.402
June 2021	172.049	166.559	5.490	3.191
July 2021	171.537	166.046	5.419	3.201

Tables 5, 6, and 7 reveal a close agreement between the equilibrium model developed for NOx emission and actual plant data. Deviation ranges between 6.5% and 3.9% for Boiler A at the commissioning stage and between 3.2% and 2.3% for the same boiler at full plant load. The percentage deviation between the developed model and CEMS for Boiler B falls between 4.4% to 3.2%. Additionally, the developed model has been compared with the correlations of Lewis (1991) and Bakken and Skogly (1995), as shown in Table 8.

Source	NOx Emission (ppm)	Deviation (ppm)	Percentage error (%)
April 2021 emission data	132	0	0
Developed model	127.737	4.263	3.230
Lewis, correlation	105.522	26.478	20.059
Bakken and Skogly, correlation	110.488	21.512	16.3

The accuracy of the NOx model developed in this study is evident, with the lowest deviation from plant data compared to other correlations from literature.

Effect of Temperature on Nox Emission

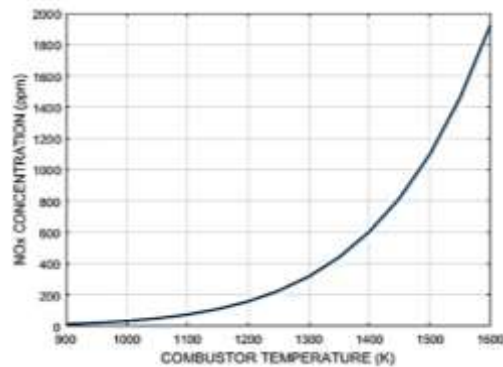


Figure 4: Effect of Temperature on NOx Emission

A graphical representation of the effect of temperature on NOx emission is presented in Figure 4.1. The graph illustrates the exponential rise of NOx emissions with an increase in combustion temperature. At 1000K, the concentration of NOx is only 32.34 ppm, while at 1600K, the concentration increases to 1926 ppm. The flame temperature must be carefully monitored to ensure that NOx concentration in the exhaust gases is kept within acceptable limits.

Effect of N2 Concentration on NOx emission

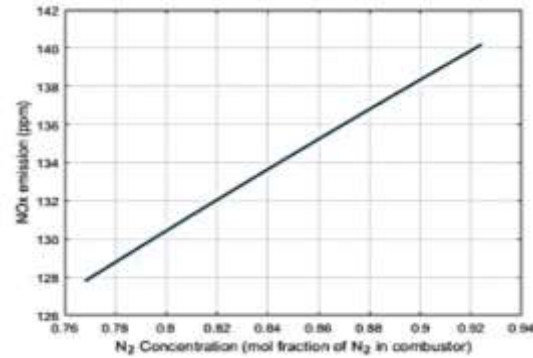


Figure 5: Effect of N2 Concentration on NOx emission

Figure 5 depicts the effect of increased N2 concentration in the combustion chamber on NOx emission. The relationship between N2 molar concentration and NOx formation is nearly linear, suggesting that reducing the concentration of N2 in the flue gas can help decrease NOx production. Additionally, when N2 concentration becomes zero, as indicated by Equation (19), no NOx will be formed, emphasizing the potential of using oxygen for combustion to eliminate NOx formation.

Other Factors Worthy of Consideration

The thermal equilibrium model developed in this study assumes sufficient residence time to reach equilibrium conditions, supported by the fast formation of NOx as confirmed by Lefebvre and Ballal (2010).

Limitation of Work

The major limitations of the models developed in this research project include:

1. The models did not account for machine degradation.
2. The models are basically applicable to lean combustors with combustion temperatures within the range of 900K to 1600K (627°C – 1327°C).
3. The accuracy of the models is dependent on proper mixing of fuel and air; implying that there is no local richness in the combustor.

Conclusions and Recommendations

Conclusions

A parametric emission model for boiler combustion has been successfully developed in this research, showing good agreement between an industrial combustor and the developed model. The model's reliance on fuel composition widens its range of applicability. The study confirms that, for boiler combustors operating in lean fuel/air mixtures, NO_x is the major pollutant of consideration. Combustor temperature significantly influences NO_x formation, with a compromise needed between cycle efficiency and combustor outlet temperature.

Recommendations

1. **Flame Temperature Reduction:** Considering the impact of excess air on flame temperature and NO_x production, future studies should explore the potential of water and steam injection into the combustor for quenching flame temperature.
2. **Oxygen-Enriched Combustion:** Investigating the use of oxygen-enriched air for combustion processes is recommended, as it can reduce the amount of nitrogen available for NO_x formation.
3. **Alternative Control Technologies:** With recent advancements in metallurgical engineering enabling higher combustion temperatures, future work should focus on cost-effective alternative control technologies for NO_x emission.

References

- Coykendall, L. H., Ta-, C., Boiler, P., Information, E., & Coykendall, L. H. (2012). Formation and Control of Sulfur Oxides in Boilers FORMATION and CONTROL of SULFUR OXIDES in BOILERS. *Environmental Science & Technology*, 2470(1962), 2–6. <https://doi.org/10.1080/00022470.1962.10468129>
- Davison, J., Bernard, Y., Borken-Kleefeld, J., Farren, N. J., Hausberger, S., Sjödin, Å., Tate, J. E., Vaughan, A. R., & Carslaw, D. C. (2020). Distance-based emission factors from vehicle emission remote sensing measurements. *Science of the Total Environment*, 739, 139688. <https://doi.org/10.1016/j.scitotenv.2020.139688>
- Himmelblau, D. M., & R., J. B. (2004). *Basic Principles and Calculations in Chemical Engineering*. Prentice Hall. www.phptr.com
- Jeevan, K., Reddy, T. K., & Reddy, T. K. (2022). Geographical air pollution prediction. *Environmental Pollution*, 13(07), 251–256.
- JusticeNews. (2016). Volkswagen to Spend Up to \$14. Protection, Consumer Environment. <https://www.justice.gov/opa/pr/volkswagen-spend-147-billion-settle-allegations-cheating-emissions-tests-and-deceiving>
- Kitto, J. B., & Beach, W. P. (2017). Air Pollution Control for Industrial Boiler Systems. September.
- Kusek, J. Z., & Rist, R. C. (2004). *10 Steps to Result-Based Monitoring and Evaluation*.
- Li, T., Yu, Y., Sun, Z., & Duan, J. (2022). A comprehensive understanding of ambient particulate matter and its components on the adverse health effects based on epidemiological and laboratory evidence. *Particle and Fibre Toxicology*, 1–25. <https://doi.org/10.1186/s12989-022-00507-5>
- Lu, P. (2021). iMedPub Journals Pollution and Ecology. 2021.
- Manisalidis, I., Stavropoulou, E., & Stavropoulos, A. (2020). Environmental and Health Impacts of Air Pollution : A Review. *Frontiers in Public Health*, 8(February), 1–13. <https://doi.org/10.3389/fpubh.2020.00014>
- Ness, J. E., Ravi, V., & Heath, G. (2021). An Overview of Policies Influencing Air Pollution from the Electricity Sector. *Environmental Science & Technology*, August.
- Okedere, O. B., Elehinafe, F. B., Oyelami, S., & Ayeni, A. O. (2021). Drivers of anthropogenic air emissions in Nigeria - A review. *Heliyon*, 7(February), e06398. <https://doi.org/10.1016/j.heliyon.2021.e06398>
- Risano, A. Y. E., & Prabowo, A. D. (2021). Analysis of the ambient air environment of the steam power plant industry. *IOP Conference Series: Materials Science and Engineering*, 1125(012086). <https://doi.org/10.1088/1757-899X/1125/1/012086>
- Signorelli, S., Sainz, M., Tabares-da Rosa, S., & Monza, J. (2020). The Role of Nitric Oxide in Nitrogen Fixation by Legumes. *Frontiers in Plant Science*, 11(June), 1–14. <https://doi.org/10.3389/fpls.2020.00521>
- USAID. (2012). Nigeria's Climate Change Fact Sheet. *USAID Nigeria Climate Change Fact Sheet*, 3. [https://www.usaid.gov/sites/default/files/documents/Climate Change Fact Sheet - NIGERIA FINAL FORMAT2.pdf](https://www.usaid.gov/sites/default/files/documents/Climate%20Change%20Fact%20Sheet%20-%20NIGERIA%20FINAL%20FORMAT2.pdf)
- USEPA. (2022)